Explainable Supervised Domain Adaptation

Vidhya Kamakshi *, Narayanan C Krishnan †
* *Department of Computer Science and Engineering, Indian Institute of Technology Ropar,* Rupnagar - 140001, Punjab, India.
Email: 2017csz0005@iitrpr.ac.in
† *Department of Data Science, Indian Institute of Technology Palakkad,* Palakkad - 678557, Kerala, India.
Email: ckn@iitpkd.ac.in

***Abstract*—Domain adaptation techniques have contributed to the success of deep learning. Leveraging knowledge from an auxiliary source domain for learning in labeled data-scarce target domain is fundamental to domain adaptation. While these techniques result in increasing accuracy, the adaptation process, particularly the knowledge leveraged from the source domain, remains unclear. This paper proposes an explainable by design supervised domain adaptation framework - XSDA-Net. We integrate a case-based reasoning mechanism into the XSDA-Net to explain the prediction of a test instance in terms of similar-looking regions in the source and target train images. We empirically demonstrate the utility of the proposed framework by curating the domain adaptation settings on datasets popularly known to exhibit part-based explainability.**

***Index Terms*—Explainable by design, Interpretable ML, Explainable AI, Domain Adaptation, Explainable Domain Adaptation**

I. Introduction

Deep learning has seen great successes in the recent past [1]–[3] with the availability of large datasets [4]. However, acquiring labeled data is an expensive and time-consuming process. Harnessing a deep classifier trained on related large labeled datasets does not generalize well on the dataset of interest where limited labeled data is available due to the changes in data distribution, often called domain shift [5]. This shift may be due to differences in the marginal distribution of features or class label-based conditional distribution. Domain Adaptation encompasses techniques that help bridge the domain shift between the source and target domains. Domain adaptation has helped to learn accurate models in many critical situations where limited data is available in various tasks like image classification, activity recognition, sentiment analysis, indoor localization.

Despite such state-of-the-art accuracies, the deep models are not readily adopted in all application domains. The opaqueness of a deep network's internal mechanism is a contributing factor to its hesitancy in adoption [6]. Moreover, the right to explanation act by EU has made it mandatory to provide explanations to the users involved in the decisions made by the AI systems, leading to the development of mechanisms for explaining deep networks. Recent work is on explaining a general-purpose classifier [7]–[9]. However, not much attention is given to explaining a domain-adapted classifier where knowledge from two domains is leveraged [10]–[12].

We propose a framework that incorporates explainability by design into the domain-adapted classifier. We assume that a set of prototypical features describes a given class's instances. We aim to learn these prototypical features in a latent space where domain-invariance is achieved through supervised domain adaptation. We look for similar features in a test image to predict the class label by leveraging the learned domain-invariant prototypical features. This prediction can be explained in a case-based reasoning fashion. A sample explanation expected from our model is shown in Figure 1. The prototypical features detected in the test image are shown in various colored rectangles. The top and bottom rows show the source and target domain prototypes, respectively, that are most similar to the prototypes detected in the test image. The contribution to a label's output is computed as a linear combination of the similarity scores, where the linear coefficients are learned during the training procedure. Contribution to each class is calculated, and a softmax will be applied to obtain the corresponding class probabilities. Thus, we can build a model that transparently unearths the whole reasoning pipeline.

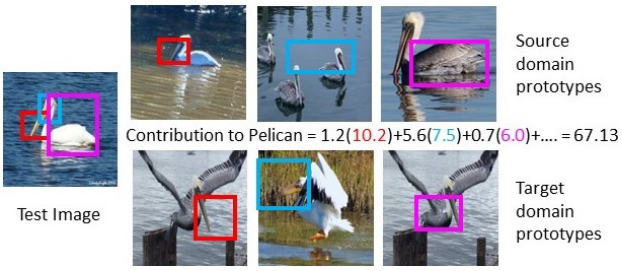

Fig. 1. [Best viewed in color] Sample explanation

The main contributions of this paper are:

- We propose a method that integrates explainability by design into a domain adaptation framework.
- We adopt a case-based reasoning style to explain a prediction based on class-specific characteristic prototypical features identified in the given test image.
- We curate domain adaptation settings using datasets commonly used in explainability literature to validate our framework's utility experimentally.

II. Related work

Supervised domain adaptation refers to the umbrella of techniques that utilize a source domain $\mathcal{D}^s = \{x_i, y_i\}_{i=1}^{N^s}$ with abundant labelled examples to learn a classifier for the target domain denoted by $\mathcal{D}^t = \{x_i, y_i\}_{i=1}^{N^t}$ with limited labelled examples. The source and target domains differ in the underlying marginal and conditional distributions. Most supervised domain adaptation approaches [13], [14] perform class-wise alignment such that the instances are clustered based on class labels ignoring domain differences which aid a classifier to learn a decision boundary that separates them. The supervised domain adaptation approaches can be categorized into discrepancy-based and adversarial techniques. In Discrepancy-based techniques [15]–[17], a discrepancy measure indicative of the domain gap is minimized, leading to the domains getting aligned closer. The same classifier trained on the source domain may then be reused to classify the target domain instances, or a new classifier can be trained using the aligned source and target labeled instances. The adversarial techniques utilize the GAN principle to align the domains. The feature extractor part of the network acts as a generator. A domain discriminator that aims to distinguish source and target domains provides feedback to the generator to generate domain invariant features [18], [19]. These domain invariant features generated for the target domain instances can then be passed through the classifier learned using the labeled source domain instances to perform classification. However, all the state-of-the-art supervised domain adaptation techniques are not interpretable. The aspects of the source and target domains focused by the classifier remain a mystery. The proposed work aims to demystify this process by integrating explainability into the design of the domain adaptation framework.

Research in explainable AI can be broadly categorized into Posthoc and Antehoc methods. In Posthoc methods, the pretrained black-box model is untouched, and a different algorithm is applied to explain its working. The feasibility constraints of early Posthoc approaches based on perturbation [20] and Activation Maximization(AM) [21] made it challenging to faithfully explain the black-box. Model-agnostic approaches [22]–[24] while can explain any model, require pre-processing (often impractical) of the input images for explaining image classification networks. Early model-specific Posthoc approaches [7], [8] highlighted a blob of an image deemed relevant by the model. Newer approaches aim to explain the network's decision in terms of human interpretable concepts [25]–[29].

Antehoc approaches incorporate explainability into the model in the design phase. Attention mechanism [30], one of the early approaches that incorporated explainability during the training phase, fail to consider network layers succeeding the attention layer [31], [32]. Antehoc models may also be obtained by making modifications in an existing architecture [33]. Li et al. [34] propose a case-based learning mechanism to learn characteristic prototypes based on whose similarity classification is performed. Chen et al. [9] propose to learn class-specific prototypical parts (ProtoPNet) to understand the reasoning process for each class in greater detail. Hase et al. [35] perform hierarchical classification by applying the ProtoPNet framework [9] at each level in the hierarchy. Wang et al. [36] suggests an alternative framework similar to ProtoPNet [9] employing the technique of projection to a subspace encompassing class-specific concepts to aid classification.

Despite advancements individually in domain adaptation and explainable AI, less focus is given to explaining the working of domain-adapted classifiers. Szabó et al. [11] uses Activation Maximization (AM) [21] to visualize the filters during the transfer learning process. However, the use of AM makes the explanation less useful for non-experts. Hao & Zheng [12] use a GAN to understand features that help achieve domain invariance. However, using a black-box to explain a black-box makes the explanation less faithful. Neyshabur et al. [37] perform a detailed analysis to unearth the role of feature reuse and pretrained weights during the process of fine-tuning. In contrast, we propose to explain the domain-adapted classifier using class-specific prototypical parts. The prototype discovery process is tightly integrated into the domain adaptation module, thus realizing explainability by design to leverage the model's knowledge gained from the data to generate the explanations.

III. Methodology

The architecture of the proposed explainable supervised domain adaptation network (XSDA-Net) is illustrated in Figure 2. An input image x is passed through a convolutional backbone f. The feature map $f(x)$ obtained from the convolutional backbone is of dimensions $H \times W \times F$.

The feature maps $f(x)$ are passed through the explanatory backbone g consisting of the prototype layers corresponding to the source and target domains g^s and g^t respectively. Every class has C prototypes of dimensions $1 \times 1 \times F$ per domain. p_{kl}^s denotes the l^{th} source prototype of the k^{th} class and p_{kl}^t denotes the l^{th} target prototype of the k^{th} class. We first describe how to classify a target test image using the trained XSDA-Net. Learning the XSDA-Net is described later.

Let $P_k^s = \{p_{kl}^s\}_{l=1}^C$ and $P_k^t = \{p_{kl}^t\}_{l=1}^C$ denote the set of source and target prototypes for k^{th} class respectively. For each source prototype p_{kl}^s, there is a paired target prototype p_{kj}^t such that $||p_{kl}^s - p_{kj}^t||_2^2$ is the least among the set of target prototypes, $\{p_{ki}^t\}_{i=1}^C$. Given the feature map $f(x)$, we first compute the Euclidean distance between each $1 \times 1 \times F$ patch in $f(x)$ with all the source and target prototypes. Let D_{kl}^s and D_{kl}^t denote the $H \times W$ matrices representing the distance of each of the $H \times W$ patches in $f(x)$ from p_{kl}^s and p_{kl}^t prototypes of the source and target respectively. The convex combination of the distance matrices $\mathcal{W}_{kl} = \alpha D_{kl}^s + (1-\alpha) D_{kj}^t$ that covers information from both source and target domains is converted into a similarity score by means of a monotonically increasing function given by $S_{kl} = \log\left(\frac{\mathcal{W}_{kl}+1}{\mathcal{W}_{kl}+\epsilon}\right)$ (where ϵ is a small non-zero value used to avoid numerical instability during the element-wise division operation). Each element in

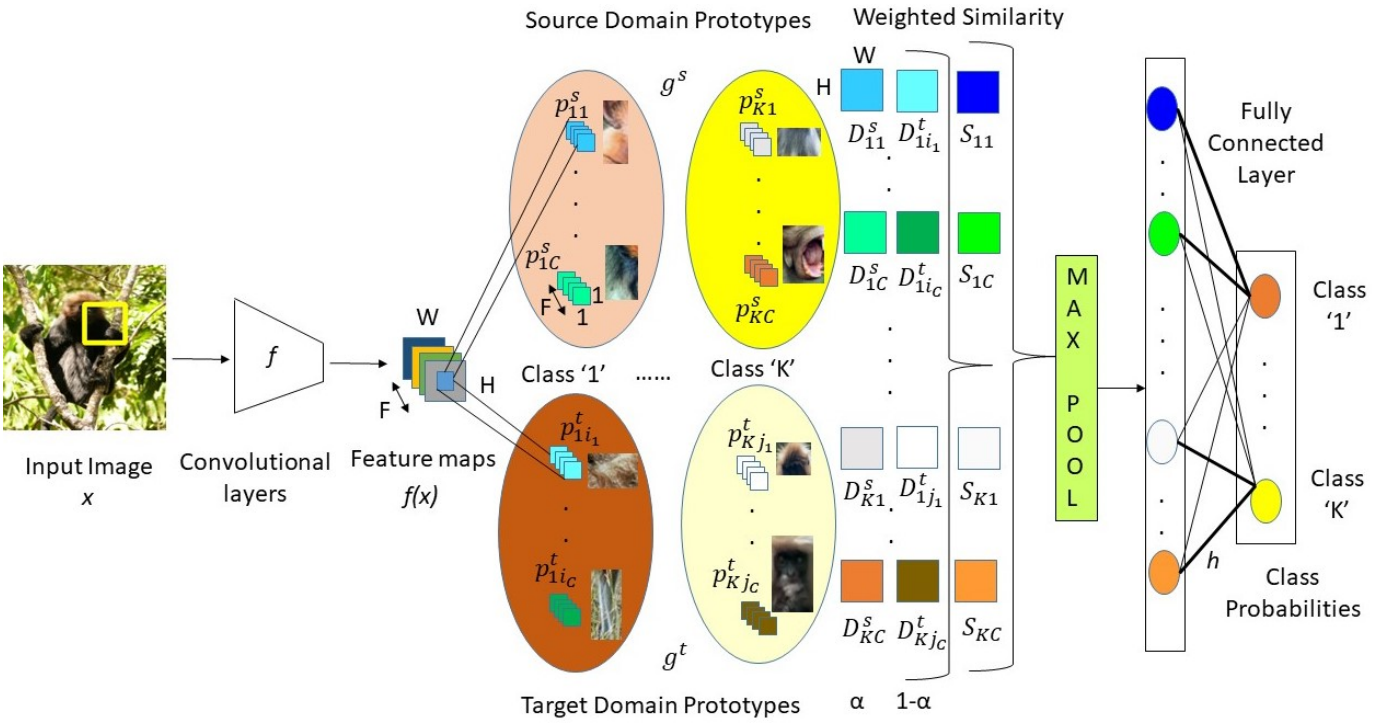

Fig. 2. [Best viewed in color] XSDA-Net Architecture

S_{kl} denotes the similarity of each patch in $f(x)$ with respect to the learned prototype. The maximum similarity value obtained through max-pool layer is passed to a fully connected linear layer h that outputs the classification probabilities. Max pool is used because the dominant presence of a pattern similar to that of the learned prototypes has to impact classification irrespective of the location of the pattern. Furthermore, S_{kl} can be upsampled to visualize the region in the test image with the maximum similarity. The regions in the test image with the maximum similarity to the source and target prototypes form part of the explanation. Thus, the XSDA-Net can be represented as a composition $h \circ g \circ f$, where f is the feature extractor, g is the prototype-based explanation backbone and h is the aggregator that performs prediction based on the interpretable components extracted by f and g.

A. Training Procedure

We adopt a three-phase training cycle to learn the prototype layer g comprising the source and target domain prototype set g^s and g^t respectively. In the first phase, the aim is to learn a latent space where class discriminativeness is achieved by employing different loss functions and bridging the domain gap. We initiate the other two phases concurrently at regular intervals, followed by the initial learning phase. The main aim of the second phase is to reinforce the explainability of the framework, where the learned representations are mapped onto a training image patch that will be visualized to understand the learned aspect. The third phase trains the dense layer's weights connecting the similarity vector to the output.

1) Learning explanatory latent space: We aim to learn a meaningful latent representation for the prototypes in the first phase. We want the prototypes to be class-specific discriminative image regions that aid the classification of any test instance. To instill class-specificity, we enforce that the given class k prototypes are clustered closer in the latent space. This is achieved through the clustering loss [9] applied to each domain independently $d \in s, t$, defined in equation 1.

$$\mathcal{L}_C^d = \frac{1}{N^d} \sum_{i=1}^{N^d} \min_{j:p_j \in P_{y_i}^d} \min_{z \in patches(f(x_i))} ||z - p_j||_2^2 \quad (1)$$

The clustering loss makes sure that the learned prototypical representation is closer to at least one training image patch of the corresponding domain having the same ground truth as that of the prototype.

The overall clustering loss is given as a weighted combination of clustering loss at each domain as given in equation 1.

$$\mathcal{L}_C = \beta_s \mathcal{L}_C^s + \beta_t \mathcal{L}_C^t \quad (2)$$

We also want the prototypes of a given class k to be far apart from the prototypes of other classes $k^{'} \neq k$. This is enforced by means of a separation loss on the prototypes of both the source and target domains $d \in s, t$, defined as

$$\mathcal{L}_S^d = -\frac{1}{N^d} \sum_{i=1}^{N^d} \min_{j:p_j \notin P_{y_i}^d} \min_{z \in patches(f(x_i))} ||z - p_j||_2^2 \quad (3)$$

The separation loss makes sure that the learned prototypical representation is farther from all training image patches of the

corresponding domain having ground truth class labels other than that of the prototype.

The overall separation loss is given as a weighted combination of the separation loss for each domain as given in equation 3.

$$\mathcal{L}_S = \gamma_s \mathcal{L}_S^s + \gamma_t \mathcal{L}_S^t \tag{4}$$

We hope to learn unique prototypes by enforcing that the representation corresponding to a given prototype is distinct and far apart from that of other prototypes. This is enforced through a distinction loss as given in equation 5.

$$d \in \{s,t\} \mathcal{L}_D^d = -\frac{1}{N^d} \sum_{i=1}^{N^d} \sum_{j:p_j \in P_{y_i}^d} \min_{z_j \in patches(f(x_i))} ||z_j - p_{j'}||_2^2 \tag{5}$$

The distinction loss ensures that all prototypes of a given class are not clustered around the same image patch.

The overall distinction loss is given as a weighted combination of distinction loss at each domain as in equation 6.

$$\mathcal{L}_D = \delta_s \mathcal{L}_D^s + \delta_t \mathcal{L}_D^t \tag{6}$$

Cross-entropy loss is minimized to improve the classification output. The fully connected layer weights are initialized such that the weights connecting the prototype to its corresponding class are kept 1, and the rest are kept as -0.5. This facilitates the model to learn that the stronger presence of the prototypes should enhance the prediction probability for its corresponding class. The domain specific cross entropy loss and the overall loss is defined as

$$d \in \{s,t\} \mathcal{L}_{CE}^d = \frac{1}{N^d} \sum_{i=1}^{N^d} CrsEnt(h \circ g \circ f(x_i), y_i) \tag{7}$$

$$\mathcal{L}_{CE} = \omega_s \mathcal{L}_{CE}^s + \omega_t \mathcal{L}_{CE}^t \tag{8}$$

Minimizing domain adaptation loss $\mathcal{L}_{DA}$ aligns the prototype representations of source and target domains in the latent space. In this paper, we leverage the d-SNE technique [38] to perform supervised domain alignment. The loss is applied to the prototypes of each domain. This loss $\mathcal{L}_{DA}$ is given in equations 9 and 10. The main idea is to separate the classes in the prototypical latent space by minimizing the maximum distance among the prototypes belonging to the same class (i.e., minimizing the maximum intra-class prototype distance) and maximizing the minimum distance among prototypes of different classes (i.e., maximizing the minimum inter-class prototype distance) across the domains.

$$d \in \{s,t\} \mathcal{L}_{DA} = \frac{1}{K \times C} \sum_{k=1}^{K} \sum_{l=1}^{C} \mathcal{L}_{DA}(p_{kl}^d) \tag{9}$$

where

$$\mathcal{L}_{DA}(p_{kl}^d) = arg\max_j ||p_{kl}^d - p_{kj}^{d'}||_2^2 - \forall_{y \neq k} arg\min_i ||p_{kl}^d - p_{yi}^{d'}||_2^2 \tag{10}$$

$d, d' \in \{s,t\}$ denotes source and target domains and $d' \neq d$.

The overall objective function comprising of all the loss terms discussed above as given in equation 11 is minimized using an Adam optimizer [39]

$$\mathcal{L} = \mathcal{L}_C + \mathcal{L}_S + \mathcal{L}_D + \mathcal{L}_{CE} + \kappa \mathcal{L}_{DA} \tag{11}$$

2) Projecting the Prototypes: The main aim of this phase is to map the learned prototype vectors to humanly understandable train image patches. We assign the prototypical representations learned to the nearest patch among the train images of the corresponding class of the domain under consideration. This can be mathematically represented as $p_{kl}^s \leftarrow arg\min_{z \in patches(f(x)); x \in \mathcal{D}_k^s} ||z - p_{kl}^s||_2$ and $p_{kl}^t \leftarrow arg\min_{z \in patches(f(x)); x \in \mathcal{D}_k^t} ||z - p_{kl}^t||_2$. A rectangular box covering the maximally activated image region yields the visualization of the prototype.

3) Learning the classifier: The fully connected layer will use the prototypical representations modified in the projection phase to perform classification. Thus the main aim of the third phase, post the projection phase, is to finetune these fully connected layer weights. The feature extractor f and the explanatory backbone g are frozen in this phase. The fully connected layer weights are finetuned to accommodate the changes due to the projection phase. Sparse connection weights are encouraged employing a L_1 regularizer. As the contribution to a class is a weighted combination of the similarity scores, sparsity in weights results in fewer prototypes contributing more to the final output.

B. Gradual training

We use a warm-start training strategy, where the feature extraction backbone f is initialized and frozen for a few epochs, initially using a standard pretrained network (VGG, ResNet). The explanatory backbone g and the fully connected layer h of XSDA-Net are trained, utilizing the knowledge encoded in the pretrained weights. Further, learning the prototypes is like picking a vector blindfolded in the latent space. However, in the end, we must map it back to the training images for explainability. Theoretically, the entire latent space can be searched, but we restrict the search to only the subspace containing the training image features by executing the projection phase every ρ epochs.

IV. Experiments

A. Datasets

We demonstrate explanations generated by XSDA-Net using two datasets (Birds and Monkeys) commonly used to study explainable AI algorithms. The datasets contain animal images characterized by distinct concepts corresponding to different image regions, serving as ideal candidates to validate the XSDA-Net. The domain differences in the prevalent domain adaptation datasets are on finer features like color and textures [12]. Domain expertise is required to understand such finer feature-based explanations. In contrast, our framework generates readily interpretable explanations based on parts or regions of the image.

1) Birds dataset: We use eight bird classes present in both Imagenet [4] and CUB [40] datasets. A few sample instances from the two domains are shown in Figure 3. The bird images from the Imagenet and CUB are considered as source and target domains, respectively. The Imagenet dataset has more than 1000 images per class, while the CUB dataset has at most 180 images per class. The target domain train and validation splits each has ten images per class, and the rest are part of the test split.

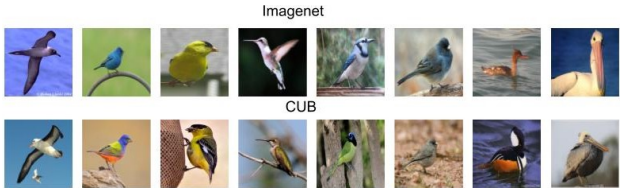

Fig. 3. [Best viewed in color] Birds dataset Visualization. Each column depicts a class.

2) Monkeys dataset: We use seven classes that are present in both Imagenet and monkey species classification datasets obtained from Kaggle. A few sample instances from the different domains are shown in Figure 4. Like the previous dataset, Imagenet with more than 1000 images per class serves as the source domain. The Kaggle dataset with at most 270 images per class is the target domain. The train and validations splits of the target domain each have ten images per class, and the rest are part of the test split.

Fig. 4. [Best viewed in color] Monkeys dataset Visualization. Each column depicts a class.

The hyper-parameters used to train the explainer were $C = 10$, $\alpha = 0.5$, $\beta_s = \beta_t = 10$, $\gamma_s = \gamma_t = -0.08$, $\delta_s = \delta_t = -0.01$, $\omega_s = \omega_t = 50$, $\kappa = 20$, $\rho = 10$. The optimal values were obtained through extensive cross validation experiments involving only the train and validation splits.

The test accuracy of the black-box domain adapted VGG16 classifier without the explanation module is 96.2% and 98.3% for the birds and monkeys dataset, respectively. In contrast, the explainable by design domain adaptation framework, XSDA-Net's accuracy is 92.4% and 96.8%, respectively. The marginal drop in the performance due to architectural modifications is tolerable considering the significant benefits of extracting interpretable explanations.

B. Correct Classification

We illustrate and discuss explanations generated by the XSDA-Net for a few correctly classified instances from the target domain. Figure 5 presents explanations for eight test instances along with the reasoning pipeline for the classification. For brevity, the illustrated prototype pairs from the source and target train set (marked by the colored rectangles) are restricted to the top 3 prototypes ranked by the similarity scores. A salient observation is the close resemblance of the prototype pairs from the source and target domains. The contribution score of source and target prototype pair (represented using the same colored rectangle) to a particular class computed as a weighted combination of the calculated similarity scores is displayed using the same color. The weights of this combination (numbers displayed in black) are learned during the training phase. In these examples, as we can see, despite visual differences, the corresponding body parts are aligned between the source and target domains due to the explicit training scheme. The test images are correctly classified due to the high similarity with the aligned prototypes from the source and target train sets. For example, body parts such as beaks and wings are used by the model to correctly classify *bunting* and other bird species. Similarly, the model considers face, body, and limbs among the top prototypes for correctly classifying *patas* and other monkey species. It is also interesting to note that a prototype for the *merganser* bird species is the background water. While the background may not be a characteristic for this class, the explanations highlight the bias in the dataset (all *merganser* images have water in the background). Despite lowered performance due to architectural modifications, our explainable by design framework discovers the underlying learning and case-based reasoning process that is impossible from a black-box pipeline.

C. Misclassification

Figure 6 illustrates the explanations for a few misclassified examples. A justifiable visual similarity is seen between the detected test image regions and the learned prototypes of both predicted and ground truth classes. Due to incorrect assessment of contribution scores, misclassification has occurred. Especially for the *marmoset* image that is misclassified as *capuchin* and *bunting* image that is misclassified as *hummingbird*, we see that the model assessed a higher similarity with the background, considering it a part of test instance, leading to the misclassification. Also, looking at the paired prototypes, we see that despite visual differences between species in both domains, due to our explicit training scheme enforcing part-based alignment, the corresponding body parts are aligned. This empirically shows the effectiveness of XSDA-Net as an explainable domain adaptation network.

V. Conclusion

Thus we have proposed the XSDA-Net that can unearth the reasoning pipeline in a classifier aligned via domain adaptation. XSDA-Net uses case-based reasoning to explain the output of the domain adapter classifier. Specifically, it explains the model's output for a test image in terms of highly similar prototypical regions from source and target train image pairs, along with the contribution of the similarity to the final

Fig. 5. [Best viewed in color] Explanations for a few correctly classified test instances. The test image regions (colored rectangles in the image in the first column) map to the regions in the source and target image regions (successive image pairs with rectangles of the same color). The source and target image prototype pairs are sorted based on the similarity to the test image region. The fully connected layer weight connecting the prototype to the corresponding class is in black. The contribution to the corresponding class is computed via this weighted combination.

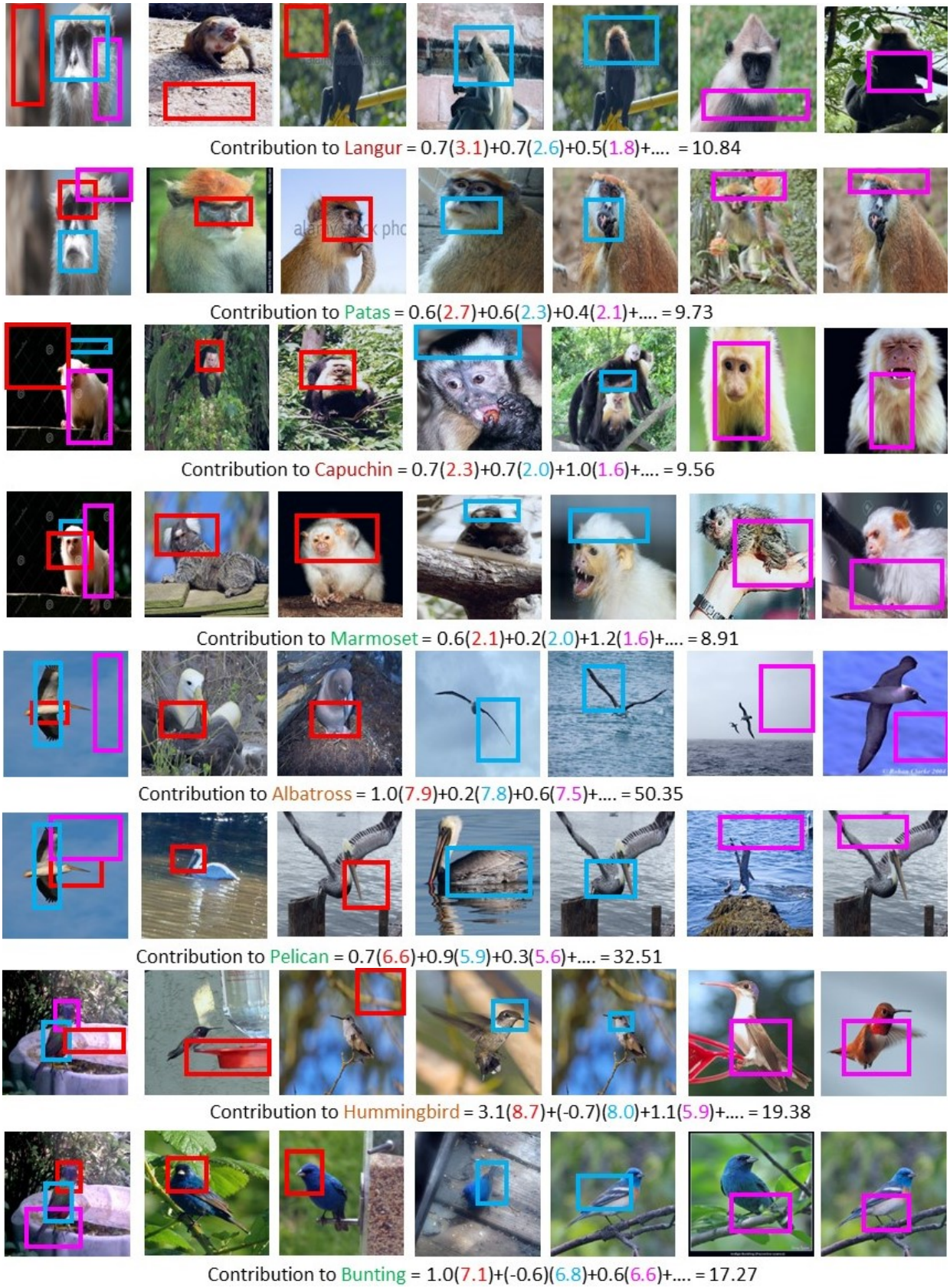

Fig. 6. [Best viewed in color] Misclassified images. The explanation for each misclassified instance spans across two rows. The first row shows the explanation corresponding to the class incorrectly predicted by the model whose label is given in brown color. The second row shows the explanation corresponding to the ground truth class whose label is given in green color. The test image regions (colored rectangles in the image in the first column) map to the regions in the source and target image regions (successive image pairs with rectangles of the same color). The source and target image prototype pairs are sorted based on the similarity to the test image region. The fully connected layer weight connecting the prototype to the corresponding class is in black. The contribution to the corresponding class is computed via this weighted combination.

output. Experiments on curated domain adaptation datasets illustrate the XSDA-Net's effectiveness in explaining correct and incorrect classifications despite a marginal decrease in the accuracy compared to its non-explainable counterparts.

REFERENCES

[1] A. Krizhevsky, I. Sutskever, and G. E. Hinton, "Imagenet classification with deep convolutional neural networks," in *Advances in Neural Information Processing Systems*, 2012, pp. 1097–1105.

[2] K. Simonyan and A. Zisserman, "Very deep convnets for large-scale image recognition," 2014.

[3] K. He, X. Zhang, S. Ren, and J. Sun, "Deep residual learning for image recognition," in *Proceedings of the IEEE Conference on Computer Vision and Pattern Recognition*, 2016, pp. 770–778.

[4] O. Russakovsky, J. Deng, H. Su, J. Krause, S. Satheesh, S. Ma, Z. Huang, A. Karpathy, A. Khosla, M. Bernstein *et al.*, "Imagenet large scale visual recognition challenge," *International Journal of Computer Vision*, vol. 115, no. 3, pp. 211–252, 2015.

[5] S. Kumar, V. K. Kurmi, P. Singh, and V. P. Namboodiri, "Mitigating uncertainty of classifier for unsupervised domain adaptation," *arXiv preprint arXiv:2107.00727*, 2021.

[6] Z. C. Lipton, "The doctor just won't accept that! interpretable ml symposium," in *Neural Information Processing Systems*, vol. 1711, 2017.

[7] R. R. Selvaraju, M. Cogswell, A. Das, R. Vedantam, D. Parikh, and D. Batra, "Grad-cam: Visual explanations from deep networks via gradient-based localization," in *Proceedings of the IEEE International Conference on Computer Vision*, 2017, pp. 618–626.

[8] S. Desai and H. G. Ramaswamy, "Ablation-cam: Visual explanations for deep convolutional network via gradient-free localization," in *The IEEE Winter Conference on Applications of Computer Vision*, 2020, pp. 983–991.

[9] C. Chen, O. Li, D. Tao, A. Barnett, C. Rudin, and J. K. Su, "This looks like that: deep learning for interpretable image recognition," in *Advances in Neural Information Processing Systems*, 2019, pp. 8928–8939.

[10] V. K. Kurmi, S. Kumar, and V. P. Namboodiri, "Attending to discriminative certainty for domain adaptation," in *Proceedings of the IEEE Conference on Computer Vision and Pattern Recognition*, 2019, pp. 491–500.

[11] R. Szabó, D. Katona, M. Csillag, A. Csiszárik, and D. Varga, "Visualizing transfer learning," *ICML Workshop on Human Interpretability in Machine Learning*, 2020.

[12] Y. Hou and L. Zheng, "Visualizing adapted knowledge in domain transfer," in *Proceedings of the IEEE/CVF Conference on Computer Vision and Pattern Recognition*, 2021, pp. 13 824–13 833.

[13] B. Kulis, K. Saenko, and T. Darrell, "What you saw is not what you get: Domain adaptation using asymmetric kernel transforms," in *Proceedings of the IEEE/CVF Conference on Computer Vision and Pattern Recognition*. IEEE, 2011, pp. 1785–1792.

[14] K. Saenko, B. Kulis, M. Fritz, and T. Darrell, "Adapting visual category models to new domains," in *European Conference on Computer Vision*. Springer, 2010, pp. 213–226.

[15] A. Gretton, K. M. Borgwardt, M. J. Rasch, B. Schölkopf, and A. Smola, "A kernel two-sample test," *The Journal of Machine Learning Research*, vol. 13, no. 1, pp. 723–773, 2012.

[16] B. Sun and K. Saenko, "Deep coral: Correlation alignment for deep domain adaptation," in *European Conference on Computer Vision*. Springer, 2016, pp. 443–450.

[17] W. Zellinger, B. A. Moser, T. Grubinger, E. Lughofer, T. Natschläger, and S. Saminger-Platz, "Robust unsupervised domain adaptation for neural networks via moment alignment," *Information Sciences*, vol. 483, pp. 174–191, 2019.

[18] E. Tzeng, J. Hoffman, K. Saenko, and T. Darrell, "Adversarial discriminative domain adaptation," in *Proceedings of the IEEE Conference on Computer Vision and Pattern Recognition*, 2017, pp. 7167–7176.

[19] Z. Pei, Z. Cao, M. Long, and J. Wang, "Multi-adversarial domain adaptation," in *Proceedings of the AAAI conference on Artificial Intelligence*, 2018.

[20] R. C. Fong and A. Vedaldi, "Interpretable explanations of black boxes by meaningful perturbation," in *Proceedings of the IEEE International Conference on Computer Vision*, 2017, pp. 3429–3437.

[21] A. Nguyen, A. Dosovitskiy, J. Yosinski, T. Brox, and J. Clune, "Synthesizing the preferred inputs for neurons in neural networks via deep generator networks," in *Advances in Neural Information Processing Systems*, 2016, pp. 3387–3395.

[22] M. T. Ribeiro, S. Singh, and C. Guestrin, "Why should i trust you?: Explaining the predictions of any classifier," in *Proceedings of the ACM SIGKDD International Conference on Knowledge Discovery and Data Mining*. ACM, 2016, pp. 1135–1144.

[23] R. Sharma, N. Reddy, V. Kamakshi, N. C. Krishnan, and S. Jain, "Maire-a model-agnostic interpretable rule extraction procedure for explaining classifiers," in *International Cross-Domain Conference for Machine Learning and Knowledge Extraction*. Springer, 2021, pp. 329–349.

[24] H. Lakkaraju, E. Kamar, R. Caruana, and J. Leskovec, "Faithful and customizable explanations of black box models," in *Proceedings of the 2019 AAAI/ACM Conference on AI, Ethics, and Society*, 2019, pp. 131–138.

[25] B. Kim, M. Wattenberg, J. Gilmer, C. Cai, J. Wexler, F. Viegas, and R. sayres, "Interpretability beyond feature attribution: Quantitative testing with concept activation vectors (TCAV)," in *Proceedings of the International Conference on Machine Learning*, vol. 80, 2018, pp. 2668–2677.

[26] A. Ghorbani, J. Wexler, J. Y. Zou, and B. Kim, "Towards automatic concept-based explanations," in *Advances in Neural Information Processing Systems*, 2019, pp. 9273–9282.

[27] C.-K. Yeh, B. Kim, S. Arik, C.-L. Li, T. Pfister, and P. Ravikumar, "On completeness-aware concept-based explanations in deep neural networks," *Advances in Neural Information Processing Systems*, vol. 33, 2020.

[28] A. Kumar, K. Sehgal, P. Garg, V. Kamakshi, and N. C. Krishnan, "Mace: Model agnostic concept extractor for explaining image classification networks," *IEEE Transactions on Artificial Intelligence*, 2021.

[29] V. Kamakshi, U. Gupta, and N. C. Krishnan, "Pace: Posthoc architecture-agnostic concept extractor for explaining cnns," in *2021 International Joint Conference on Neural Networks (IJCNN)*. IEEE, 2021, pp. 1–8.

[30] K. Xu, J. Ba, R. Kiros, K. Cho, A. Courville, R. Salakhudinov, R. Zemel, and Y. Bengio, "Show, attend and tell: Neural image caption generation with visual attention," in *International Conference on Machine Learning*, 2015, pp. 2048–2057.

[31] A. K. Mohankumar, P. Nema, S. Narasimhan, M. M. Khapra, B. V. Srinivasan, and B. Ravindran, "Towards transparent and explainable attention models," in *Proceedings of the Annual Meeting of the Association for Computational Linguistics*, 2020, pp. 4206–4216.

[32] W. Xu, J. Wang, Y. Wang, G. Xu, D. Lin, W. Dai, and Y. Wu, "Where is the model looking at –concentrate and explain the network attention," *IEEE Journal of Selected Topics in Signal Processing*, pp. 1–1, 2020.

[33] B. Zhou, A. Khosla, A. Lapedriza, A. Oliva, and A. Torralba, "Learning deep features for discriminative localization," in *Proceedings of the IEEE Conference on Computer Vision and Pattern Recognition*, 2016, pp. 2921–2929.

[34] O. Li, H. Liu, C. Chen, and C. Rudin, "Deep learning for case-based reasoning through prototypes: A neural network that explains its predictions," in *Proceedings of the AAAI Conference on Artificial Intelligence*, 2018.

[35] P. Hase, C. Chen, O. Li, and C. Rudin, "Interpretable image recognition with hierarchical prototypes," in *Proceedings of the AAAI Conference on Human Computation and Crowdsourcing*, vol. 7, no. 1, 2019, pp. 32–40.

[36] J. Wang, H. Liu, X. Wang, and L. Jing, "Interpretable image recognition by constructing transparent embedding space," in *Proceedings of the IEEE/CVF International Conference on Computer Vision*, 2021, pp. 895–904.

[37] B. Neyshabur, H. Sedghi, and C. Zhang, "What is being transferred in transfer learning?" *Advances in Neural Information Processing Systems*, vol. 33, 2020.

[38] X. Zhou, X. Xu, R. Venkatesan, G. Swaminathan, and O. Majumder, "d-sne: Domain adaptation using stochastic neighborhood embedding," in *Domain Adaptation in Computer Vision with Deep Learning*. Springer, 2020, pp. 43–56.

[39] D. P. Kingma and J. L. Ba, "Adam : A method for stochastic optimization," *International Conference on Learning Representations*, vol. 7, 2015.

[40] P. Welinder, S. Branson, T. Mita, C. Wah, F. Schroff, S. Belongie, and P. Perona, "Caltech-UCSD Birds 200," California Institute of Technology, Tech. Rep. CNS-TR-2010-001, 2010.